Synthesis and integration of β-Ga_2O_3 nanowires on substrates with electrodes

Author: Anna Estany Macià
*Facultat de Física, Universitat de Barcelona, Diagonal 645, 08028 Barcelona, Spain.**

Advisor: Albert Romano-Rodríguez

Abstract: Monoclinic Ga_2O_3 nanowires (NWs) have been synthesised via chemical vapour deposition by the vapour-liquid-solid mechanism on Au-sputtered fused silica substrates with Cr/Pt integrated electrodes. The grown NWs have been structurally characterised by scanning electron microscopy and their electrical characteristics have been measured in atmospheres with varying relative humidity concentrations at room temperature, proving their sensing properties.

I. INTRODUCTION

Gallium oxide (Ga_2O_3) is a transparent semiconducting oxide that can crystalize in several polymorphic forms, among which its monoclinic structure, β-Ga_2O_3, is the only stable phase up to the melting point (~1800ºC) and all other polymorphic structures turn into β-Ga_2O_3 at temperatures above 750-900ºC. This polymorph has risen interest due to its unique properties, including its ultrawide bandgap (~4.8 eV) and dielectric high breakdown field strength (8 MV/cm) [1].

β-Ga_2O_3 has recently been investigated for gas sensing applications since Fleischer and Meixner [2] first reported β-Ga_2O_3 films to be O_2-sensitive at temperatures of 900-1000ºC with sensor response times of a few seconds. Their gas sensing mechanism compares to that of other metal oxides and is based on the resistance variation due to adsorption of gas molecules on their surface.

Even though nanostructures such as nanocrystals [3] and nanorods [4] have been used in several gas sensing applications, β-Ga_2O_3 nanowires (NWs), however, are an especially promising platform as the wire length and radius can be modulated during growth and their one-dimensional structure can provide a larger surface area as compared to the same volume in bulk or thin film material. Their sensitivity towards CO and other gases has been widely demonstrated using multiple [5] and metal coated [6] β-Ga_2O_3 NWs, among others, although reported literature of their humidity sensing behaviour is scarce but reliable [7].

The supervisor's group has worked on single NWs attached to metal contacts used as electrodes, which highly complicates their manipulation as they ought to be transferred to the target system.

This study is focused on the direct growth of β-Ga_2O_3 nanowires on substrates which contain integrated metallic contacts, using Chemical Vapour Deposition (CVD) via Vapour-Liquid-Solid (VLS) mechanism. The fabricated β-Ga_2O_3 NWs have been structurally characterized using Scanning Electron Microscopy (SEM) and related techniques (EDS). Some samples have undergone an electrical characterization to determine their current-voltage characteristics and their resistance variation has been further measured in the presence of various humidity concentrations.

II. EXPERIMENTAL

A. Growth of Ga_2O_3 nanowires

Monocrystalline Ga_2O_3 nanowires have been grown in CVD method via VLS mechanism. This growth process (see Fig. 1) consists in the introduction of a liquid catalyst on top of the substrate where NWs are to be grown. The precursor of the material of the NWs is evaporated, transported and incorporated into the liquid catalyst, which under continuous gas supply, leads to supersaturation and precipitation, giving rise to NWs' growth from the nucleated seeds at the liquid-solid interface.

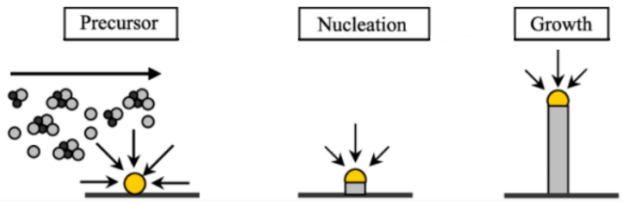

FIG. 1: Illustration of the VLS growing process [8].

First, holders are cleaned with isopropanol to remove dust and some contamination. Then, a fused silica boat containing $0{,}20 \pm 0{,}01$ g of gallium metal is placed next to an inverted alumina boat, on top of which the samples are placed. These are 5.6x10 mm^2 fused silica substrates which contain metallic electrodes made of Cr/Pt (5/150 nm). The thin Cr layer is used as an adhesion layer for Pt (Pt adheres very badly to Si or SiO_2), and for this application is much better than other adhesion layer, like titanium, as it diffuses very little inside the platinum layer. It is known that Cr thickness has no effect on the device properties. Two different metal layouts have been used: 90 pairs of interdigitated platinum electrodes (10/10 micrometre electrode/gap) with a circular shape of 3.6 mm diameter and two parallel planar electrodes of 3 mm length and 800 micrometres apart (shown in Fig. 2). These structures are connected to 2 pads at the opposite end of the substrate to allow their electrical wire bonding.

The samples have also been Au (catalyst) sputter-covered for 20 seconds to aid the VLS growth except for the pads zone, which has been left undeposited to minimise pad transformation that might compromise bonding efficiency.

* Electronic address: aestanma19@alumnes.ub.edu

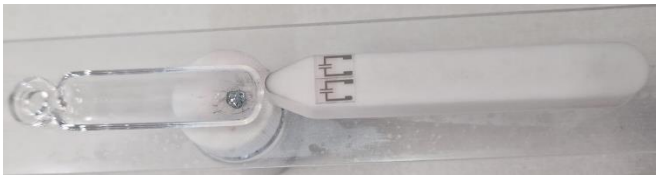

FIG. 2: Image of the experimental layout inside the quartz tube. On the left, the precursor. On the right, the substrates with parallel electrodes.

The samples are introduced in a 5 cm diameter quartz tube inside a furnace that can be heated up to 1000ºC, which is connected to a rotary vane pump and a gas injection system constituted of 4 MKS Mass-Flow controllers.

The experiment starts by pumping down the tube to minimise the presence of undesirable gases, especially water vapour, from affecting the growth process. The furnace is then heated at a constant rate until the selected temperature is reached and maintained for 1 hour, after which the system is allowed to naturally cool down.

A constant gas flow of pure Ar (5N quality) is provided during the whole process, which acts as the carrier of the precursor to the catalyst during the heating stages.

All experiments have been performed at atmospheric pressure with a constant Ar flow rate of 500 sccm, and the growth temperature has been kept between 800 and 900ºC.

B. Characterization

The obtained samples have been analysed in a Jeol 7100 Field Emission Scanning Electron Microscope (SEM), operating at 5 kV. This technique has permitted the topographical analysis of the samples by observing the grown Ga_2O_3 nanostructures using secondary electrons. This system was equipped with an Energy-Dispersive X-ray spectrometer (EDS), which has been used to observe the elemental composition of the obtained NWs, and compared with images obtained with backscattered electrons (BSE).

The electrical characterization of the samples has been carried out by measuring the current-voltage (I-V) curve with a Keithley 2602B Source Measurement Unit (SMU). This has been performed by sweeping the current to the pads and measuring the voltage drop.

Finally, the gas sensing behaviour of some samples towards different concentrations of humidity, diluted in synthetic air, has been tested using a system controlled by a home-developed LabVIEW software and composed by a self-constructed miniaturised stainless steel gas chamber connected to a gas mixer with 2 Bronkhorst mass-flow controllers (MFCs) and the Keithley 2602B SMU. The exit flow of one of the MFCs was introduced into a bubbler and its exit flow was mixed with the one of the other MFC, allowing the humidity level to be varied by changing the individual flows through the two MFC and keeping the total flow at 200 sccm (standard cubic centimetre per minute).

III. RESULTS AND DISCUSSION

A. Scanning Electron Microscopy (SEM)

Fig. 3 shows the SEM images of some of the samples fabricated, which prove the growth of Ga_2O_3 NWs on the Au-sputtered fused silica parts of the substrate. As can be seen, different lengths and densities can be appreciated as a function of the growth temperature. While Fig. 3 a) shows a dense layer of long NWs, in Fig. 3 b) they are significantly shorter. This is in agreement with previous reported studies [9], and the difference is due, mainly, to the lower vapour pressure of Ga at 800ºC, producing less gallium evaporation.

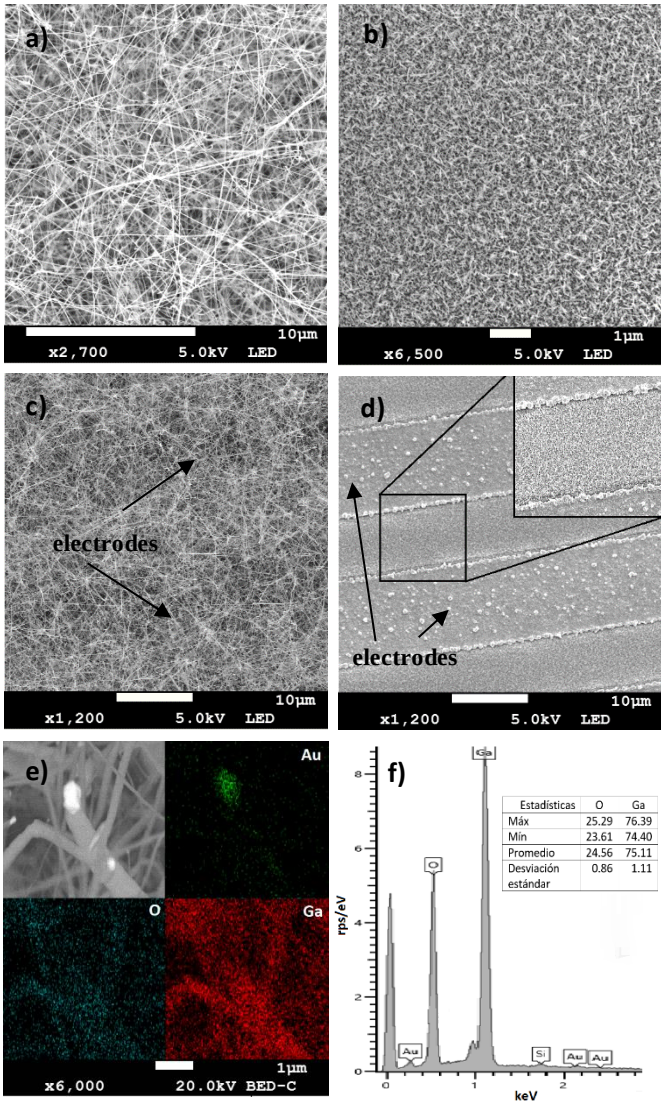

FIG. 3: SEM images of the Ga_2O_3 NWs grown on the Au-sputtered fused silica parts at a) 900ºC and b) 800ºC, and over the Au-sputtered Pt electrodes at c) 900ºC and d) at 800ºC. e) EDS map showing the NWs Au tip and f) EDS spectrum of the NWs grown at 900ºC containing the mass % of the elements present in the sample.

The growth on top of Au-sputtered Pt electrodes, however, has proved to differ from the growth on Au-sputtered fused silica. This is clearly evident in the sample grown at 800ºC

(Fig. 3 d)), but more difficult at 900ºC (Fig. 3 c)). It is well known that Au-Pt form an alloy at high temperatures, whose composition depends on the amount of both metals. In this case, because there is only a very limited amount of Au (estimated thickness of 2-3 nm) compared to the 150-nm thick Pt, all the Au will form the alloy and, consequently, the catalytic properties of Au will be lost on top of the electrodes. In the sample grown at 900ºC, due to the density and length of the NWs, this is not visible.

On the other hand, EDS has revealed droplets of Au alloys anchored at the top of the Ga_2O_3 NWs (Fig. 3 e)), which confirms that these structures have been grown following the "tip growth model" of VLS mechanism Additionally, the relative mass composition of each element in the NW has been estimated from EDS spectra (Fig. 3 d)), which is in agreement with the stochiometric Ga_2O_3.

B. Electrical characterization

The electrical measurements have been performed on the NWs grown at 900ºC with circular shaped electrodes. Even though most of the growth experiments were performed on the parallel electrodes, it was not possible to measure their resistance, as it was far above several tens of GΩ, which is the maximum value that can be measured by the SMU.

The current-voltage characteristic has been obtained by sweeping the electric current between -500 nA and 300 nA injected to the pad and measuring the resulting voltage drop. It is clear that the measured I-V curve follows a nonlinear behaviour, which indicates that the contact is not ohmic: this result can be explained by the back-to-back Schottky barrier model, which considers two different barrier heights and develops the analysis of the metal/semiconductor/metal (Pt/Ga_2O_3/Pt) configuration using the usual thermionic emission theory assumptions of the conventional Schottky model used in metal/semiconductor devices [10]. Furthermore, the observed asymmetric back-to-back behaviour indicates that the barriers that have been constructed do not present the same height. This could be caused by lack of control over the interfacial interactions between the Pt/β-Ga_2O_3 interfaces, but a further inspection of the contact interfaces should be carried out to proper analyse this behaviour.

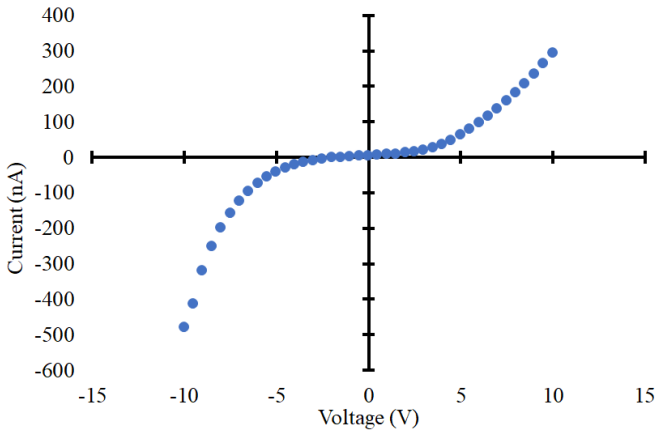

FIG. 4: V-I curve of the grown β-Ga_2O_3 NWs on the circular cell design at a temperature growth of 900ºC.

C. Gas sensing behaviour

To carry out the gas sensing measurements it is required that the sample is biased at a stable value. For this, the measurements have been performed maintaining an electric current of 3 nA, which corresponds to a voltage drop which is within the values that can be measured by the SMU.

The gas sensing measurement starts with a stabilisation phase in which the sensors are biased under the flow of dry synthetic air. Then, 15-minute pulses of wet SA with different RH concentrations have been applied, followed by 30 minutes with dry SA to allow the sensor to recover the base resistance value. During the whole process the sensor's resistance was measured.

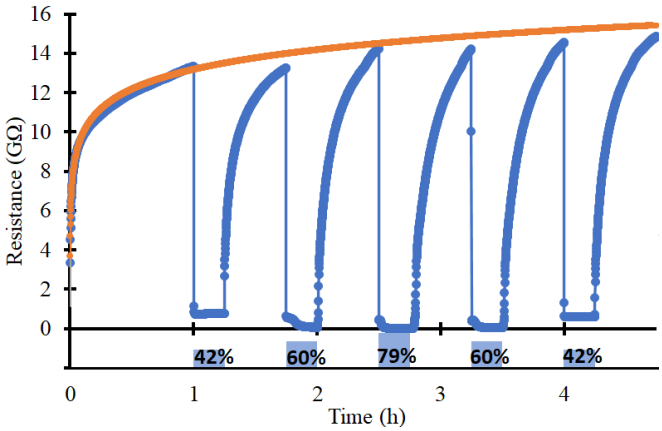

FIG. 5: Sensor resistance variation towards different RH concentrations at room temperature (blue line). The values of the concentration and the duration of the humidity pulses are indicated in the lower part. The orange line represents the extrapolation of the sensor's first stabilisation step, showing its drift and proving that longer stabilisation is required.

The obtained result, depicted in Fig. 5, shows an initial increase of resistance when applied the SA flux, which is part of the usually required stabilisation for this type of sensors, but which is not sufficient for practical applications. What is clear is that the resistance drops with the presence of humidity, in agreement with the reported behaviour of other MOX sensors to water presence [11], which reacts as a reducing gas. This behaviour can be explained by the interactions between an n-type of semiconductor, such as Ga_2O_3, and a reducing gas (Fig. 6). Initially, some atmospheric oxygen adsorbed and ionised at the semiconductor's surface gives rise to an electron depletion layer. When exposed to a H_2O reducing gas, the gas' molecules react with the adsorbed oxygen ions according to the Eq. (1) [12]:

$$H_2O + Ga_{lat-} + O_{lat}^{-} \rightarrow (HO - Ga_{lat}) + Ga_{lat} + 1e^{-} \quad (1)$$

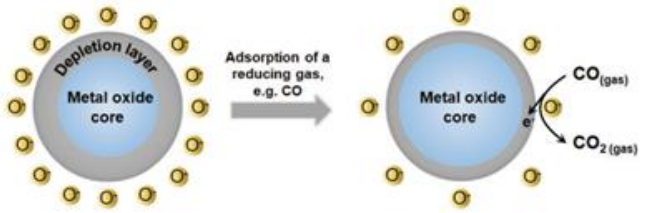

FIG. 6: Sketch of the interactions between an oxidising and a reducing gas, like CO, and the surface of an n-type semiconductor [14].

which returns one electron to the semiconductor, reduces the surface charge, gives rise to a thinner depletion layer and a larger conductive channel, and reduces the NWs resistance [13].

This phenomenon will occur until a steady state is reached, where absorption and desorption of the gas is similar and continuous, giving rise to a stable resistance.

Since a global flux of 200 sccm has been maintained during the measure, the resistance variation observed can be only assigned to the different amount of water vapour (RH) diluted in SA. Furthermore, the resistance variation is larger for increasing humidity concentrations.

The response of the sensor towards gases can be expressed in general terms as Eq. (2):

$$Response(\%) = \frac{|R_{DSA} - R_{WSA}|}{R_{DSA}} \cdot 100 \qquad (2)$$

with R_{DSA} being the base resistance (under dry SA) and R_{WSA} the steady state reached under wet SA. It is clear that in Fig. 5 the stable resistance has not been reached and a drift of the considered "base resistance" is evidenced in the measurement. This indicates that the sensor requires a much longer stabilisation time to give reliable measurements, but such long experiments are beyond the scope of this work. However, we can try to extract some parameters by extrapolating the behaviour during the first-hour stabilization, and this has been plotted (orange line) to estimate its value, which has been considered around $R_{DSA} = (15 \pm 1)\ G\Omega$, and has been used for the data analysis.

RH ± 3 (%)	R_{WSA} ±10 (MΩ)	Response ± 0,70 (%)	Recovery time ± 2 (min)
42	762	94,92	16
60	56	99,63	19
79	3	99,98	22
60	31	99,79	22
42	614	95,94	17

TABLE 1: Steady state resistance, response, and recovery time of each humidity pulse.

The estimated response of the sensor obtained for different RH concentrations (Table 1) are larger than the ones reported from single β-Ga_2O_3 NWs [15], and the sensor allows reversible measures, since pulses with the same RH have nearly the same response, with similar steady state resistance values, regardless of the order of application.

The response time of the sensor, defined as the time span between 10% and 90% of the baseline-steady state resistance variation, is below 5 seconds, the sampling frequency of the measurements, for all RH concentrations, proving the extremely fast response of the sensor to the presence of humidity in the atmosphere.

The recovery time, however, stretches to 15-22 minutes depending on the RH value. This indicates that the adsorption of the gas is much faster than the desorption, indication of a higher activation energy.

Even though the variation of the resistance increases with RH concentrations, it is clear that the sensor is very close to reach a saturation around 60-79% RH, since there is almost no difference in the variation of the resistance (see Fig. 8).

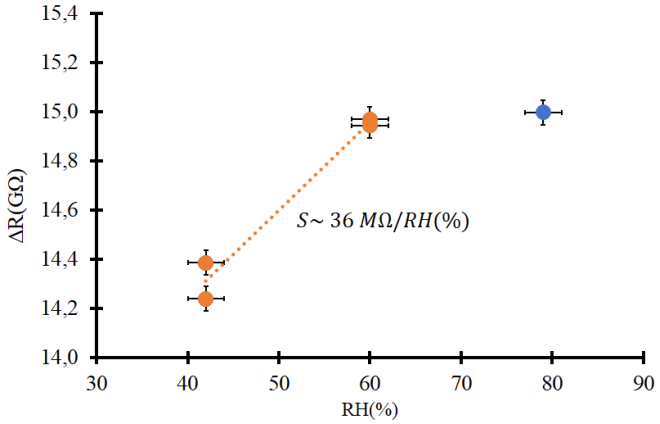

FIG. 8: Sensor resistance variation given for 42%, 60% and 79% RH.

An estimated value of the sensitivity of the fabricated sensor can be extracted from the slope of the $\Delta R - RH(\%)$ curve (excluding the saturated zone), giving an approximate value of $S\sim 36\ M\Omega/RH(\%)$. This indicates that the sensor is highly sensitive to changes in the high environment humidity range. Further measurements with different RH concentrations would be required to achieve a more accurate sensitivity, but the experimental equipment did not allow to control the humidity below 40% RH.

A final important result is that these sensing measurements have been performed at room temperature (~21°C) without the need of heating elements, which is necessary in most metal oxide-based gas sensors.[16]

IV. CONCLUSIONS

Ga_2O_3 nanowires have been directly synthesised via CVD by the VLS mechanism on fused silica substrates with Cr/Pt electrodes using Au as a catalyst and gallium metal as a precursor. The results indicate that the optimal growth temperature to achieve measurable resistive device is 900ºC, which correspond to a dense layer of long NWs, as confirmed by SEM.

The I-V measurements present a nonlinear dependence, which can be clearly interpreted by the

metal/semiconductor/metal structure of the device. At room temperature, the samples have shown an important resistance variation in the presence of high concentration of relative humidity, with a response time below 5 seconds and an estimated sensitivity of $S \sim 36\ M\Omega/RH(\%)$, but a recovery time is estimated to be tens of minutes.

Acknowledgments

I sincerely acknowledge my advisor Dr Albert Romano for his unceasing patience and support and his advice during this project, giving me the opportunity to enhance the knowledge acquired during my Physics' degree, particularly in the *Micro and Nanotechnology* and *Physical Electronics* subjects.

This project could not have been accomplished without the assistance of Dr Paolo Pellegrino, who taught me the experimental procedure to synthesize the Ga_2O_3 NWs and helped me with the initial SEM observations.

Finally, I thank my family and friends for their support and encouragement during these months.

---

[1] V. I. Nikolaev, S. I. Stepanov, A.E. Romanov and V.E. Bougrov, Single crystals of electronic materials, growth and properties, Woodhead Publ., 2019.

[2] M. Fleisher and H. Meixner, «Gallium oxide thin films: a new material for high-temperature oxygen sensors», *Sens. Actuators B Chem.*, vol. 4, pp.437-441, 1991.

[3] M. Bartic, «Mechanism of oxygen sensing on β-Ga_2O_3 single-crystal sensors for high temperatures», *Phys. Status Solidi A*, vol. 213, pp. 457-462, 2016.

[4] B. Zhang, H. Lin, H. Gao, X. Lu, C. Nam and P. Gao, «Perovskite-sensitized β-Ga_2O_3 nanorod arrays for highly selective and sensitive NO_2 Detection at high temperature», *J. Mater.Chem. A*, vol.8, pp. 10845-10845, 2020.

[5] Z. Liu, T. Yamazaki, Y. Shen, T. Kikuta, N. Nakatani and Yongxiang Li, «O_2 and CO sensing of Ga_2O_3 multiple nanowire gas sensors,» *Sens. Actuators B Chem.*, vol. 129, pp. 666-670, 2008.

[6] H. Kim, C. Jin, S. An and C. Lee, «Fabrication and CO gas-sensing properties of Pt-functionalized Ga_2O_3 nanowires,» *Ceram. Int.*, vol. 38, pp. 3563-3567, 2012.

[7] T. Tsai, S. Chang, W. Weng, S. Liu, C. Hsu, H. Hsueh and T. Hsueh, «β-Ga_2O_3 nanowires-based humidity sensors prepared on GaN/sapphire substrate,» *IEEE Sens. J.*, vol. 13, pp. 4891-4896, 2013.

[8] M. Kumar, V.N. Singh, B.R. Mehta and J.P. Singh, «Tunable synthesis of indium oxide octahedral, nanowires and tubular nanoarrow structures under oxidizing and reducing ambients,» *Nanotechnology*, vol. 20, pp. 235-608, 2009.

[9] A. Bartomeu, «Growth of β-Ga_2O_3 nanowires via CVD using Au catalyst» (Treball de Final de Grau), Universitat de Barcelona, 2021.

[10] A. J. Chiquito, C. A. Amorim, O. M. Berengue, L. S. Araujo, E. P. Bernardo and E. R. Leite, «Back-to-back Schottky diodes: the generalization of the diode theory in analysis and extraction of electrical parameters of nanodevices,» J. *Phys. Condens. Matter.*, vol. 24, pp. 225303, 2012.

[11] L. Hrachowina, G. Domènech-Gil, A. Pardo, M. S. Seifner, I. Gràcia, C. Cané, A. Romano-Rodríguez and S. Barth, «Site-specific growth and in situ integration of different nanowire material networks on a single chip: toward a nanowire-based electronic nose for gas detection, » *ACS Sens.*, vol.3, pp. 727-734, 2018.

[12] N. Barsan, M. Schweizer-Berberich and W. Göpel, «Fundamental and practical aspects in the design of nanoscaled SnO_2 gas sensors. a status report,» *Fresenius J. Anal. Chem.*, vol. 365, pp. 287-304, 1999.

[13] S. Choopun, N. Hongsith and E. Wongrat, Nanowires Recent Advances, IntechOpen, 2012.

[14] J. Dai, O. Ogbeide, N. Macadam, Q. Sun, W. Yu, Y. Li, B.-Li- Su, T. Hasan, X. Huang and W. Huang, «Printed gas sensors,» *Chem. Soc. Rev.*, vol. 49, pp. 1756-1789, 2020.

[15] G. Domènech-Gil, I. Peiró, E. López-Aymerich, M. Moreno, P. Pellegrino, I. Gràcia, C. Cané, S. Barth and A. Romano-Rodríguez, «A room temperature humidity sensor based on single β-Ga_2O_3 nanowires,» *Proceedings*, vol.2, 2018.

[16] M. Krawczyk, P. Suchorska-Wosniak, R. Szukiewicz, M Kuchowicz, R. Korbutowicz and H. Teerycz, «Morphology of Ga_2O_3 nanowires and their sensitivity to volatile organic compounds,» *Nanotechnology*, vol. 11, 2021.